

El Niño in a warming world: Transient and equilibrium responses to enhanced atmospheric greenhouse gases

Steven J. Phipps

Climate Change Research Centre, University of New South Wales, Sydney, Australia (s.phipps@unsw.edu.au)

1. Introduction

The response of El Niño to increased atmospheric greenhouse gas (GHG) concentrations is uncertain. There is a considerable spread in El Niño behaviour between the IPCC AR4 models, with models simulating either increased or reduced El Niño variability in response to increasing GHGs (Guilyardi, 2006). However, the AR4 models were not integrated for sufficient duration to allow the equilibrium response of El Niño to enhanced GHGs to be investigated. To explore both the *transient* (short-term) and *equilibrium* (long-term) changes in El Niño characteristics, this study integrates a low-resolution coupled atmosphere-sea ice-ocean general circulation model to equilibrium for scenarios in which the atmospheric CO₂ concentration is increased to two, three and four times the pre-industrial level.

2. Climate model simulations

This study uses the CSIRO Mk3L climate system model v1.1 (Phipps, 2006). It comprises an atmospheric general circulation model with a resolution of $5.6^\circ \times 3.2^\circ$ and 18 vertical levels, an oceanic general circulation model with a resolution of $2.8^\circ \times 1.6^\circ$ and 21 vertical levels, a dynamic-thermodynamic sea ice model, and a land surface scheme with static vegetation.

A 10,000-year pre-industrial control simulation is conducted, in which the CO₂ concentration is held constant at 280 ppm. Three further transient simulations are conducted. Starting from year 100 of the control simulation, the CO₂ concentration is increased at 1% pa until it reaches 2, 3 and 4 times the pre-industrial level (560, 840 and 1120 ppm respectively). The CO₂ concentration reaches these values in years 170, 211 and 240 respectively, and is held constant thereafter. Each simulation is integrated for a total of 6,500 years, ensuring that the climate system has reached thermal equilibrium.

3. Changes in El Niño variability

The changes in the amplitude of El Niño variability are shown in Figure 1. As the CO₂ concentration increases, the initial response of the model is an increase in El Niño variability. However, once the CO₂ concentration is stabilised, there is a rapid decrease in variability within the 3× and 4×CO₂ simulations, particularly in the Niño 3.4 region. There is a further, slow decline in variability as the simulations progress towards thermal equilibrium, which is also experienced by the 2×CO₂ simulation.

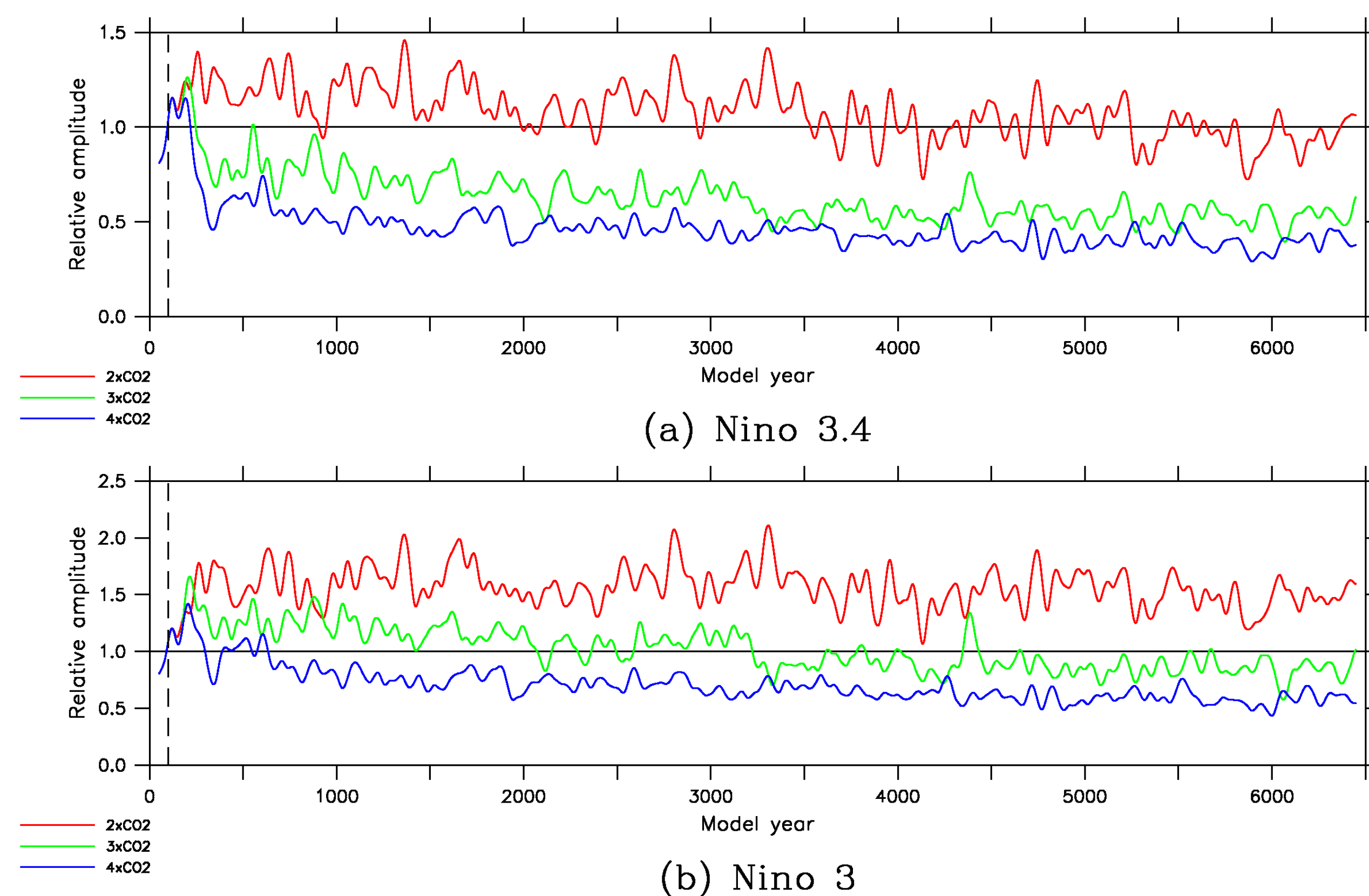


Figure 1. The amplitude of the variability in **a** the Niño 3.4 and **b** the Niño 3 SSTs, expressed relative to the amplitude in the control simulation. The values plotted represent the amplitude of the variability in the 2–7 year band, and have been smoothed using a Hann window with a width of 100 years.

It is apparent from Figure 1 that the metric used to measure El Niño variability must be chosen carefully. In the 2×CO₂ simulation, for example, the equilibrium response comprises a 5% decrease in variability in the Niño 3.4 region, but a 47% increase in variability in the Niño 3 region; the choice of metric can therefore determine both the sign and magnitude of the change.

4. Changes in ENSO dynamics

The leading principal components of sea surface temperature (SST) for each simulation are shown in Figure 2. As the CO₂ concentration is increased, the location of greatest SST variability shifts eastwards and El Niño events become increasingly confined to the eastern Pacific. This shift explains why variability in the Niño 3.4 region decreases by more than that in the Niño 3 region. Also apparent from Figure 2 is the increase in El Niño variability in the 2×CO₂ simulation, in contrast to the reduction at higher CO₂ concentrations. The El Niño mode is almost completely absent in the 4×CO₂ simulation.

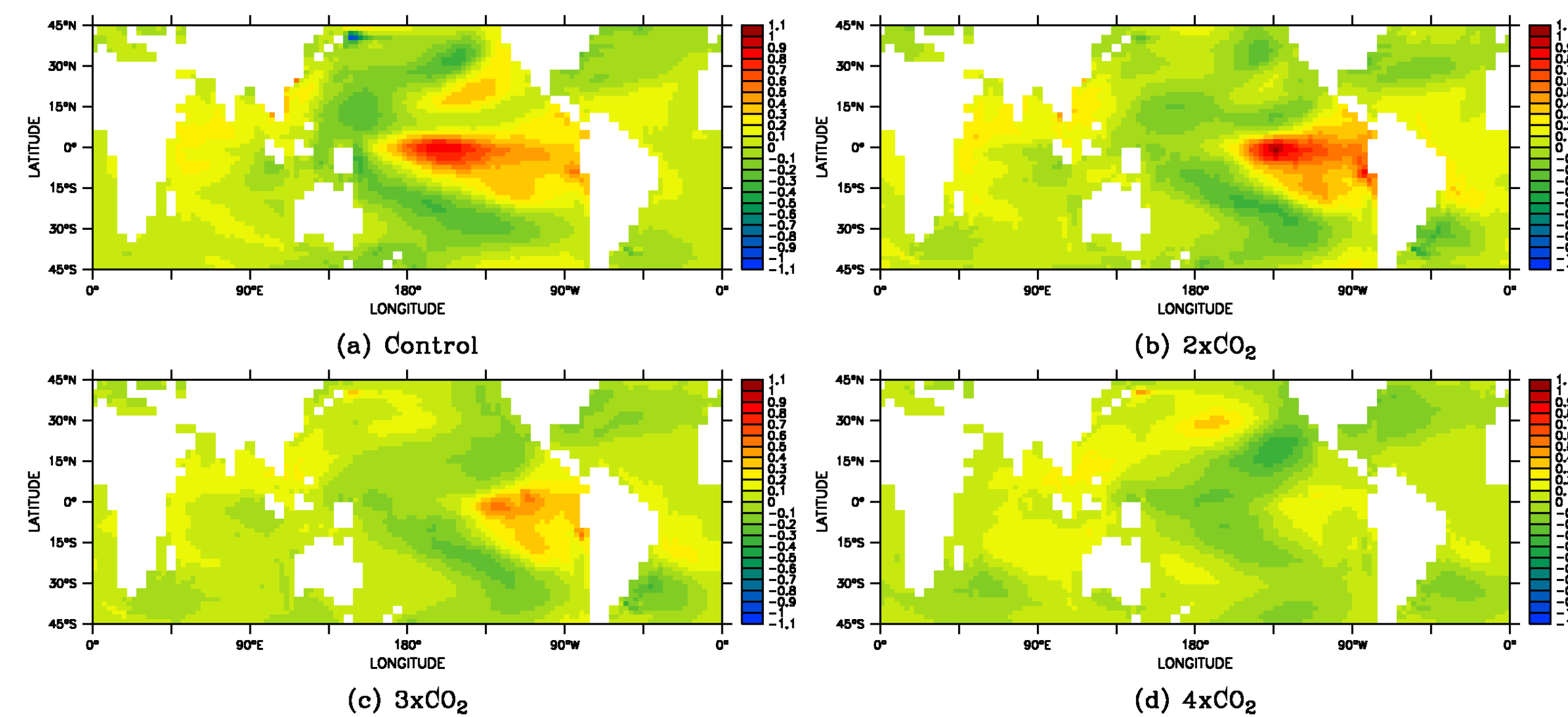


Figure 2. The leading principal components (K) of the monthly SST anomalies for **a** the control simulation, and **b–d** the equilibrated stages of the 2×, 3× and 4×CO₂ simulations respectively.

Figure 3 shows the lag correlation of the Trans-Niño Index (TNI; Trenberth and Stepaniak, 2001) with the Niño 3 SST anomaly. A positive correlation for negative lags means that the TNI leads the Niño 3 SST, and hence that the direction of SST anomaly propagation is from east to west (S-mode); the opposite means that the direction of propagation is from west to east (T-mode) (Guilyardi, 2006).

The control simulation exhibits a hybrid mode, shifting between S-mode and T-mode on decadal timescales in a manner which is consistent with 20th century observations. However, the dynamics of El Niño events change in response to elevated CO₂. S-mode is entirely absent from the transient simulations, and El Niño events become increasingly rapid as the CO₂ concentration is increased.

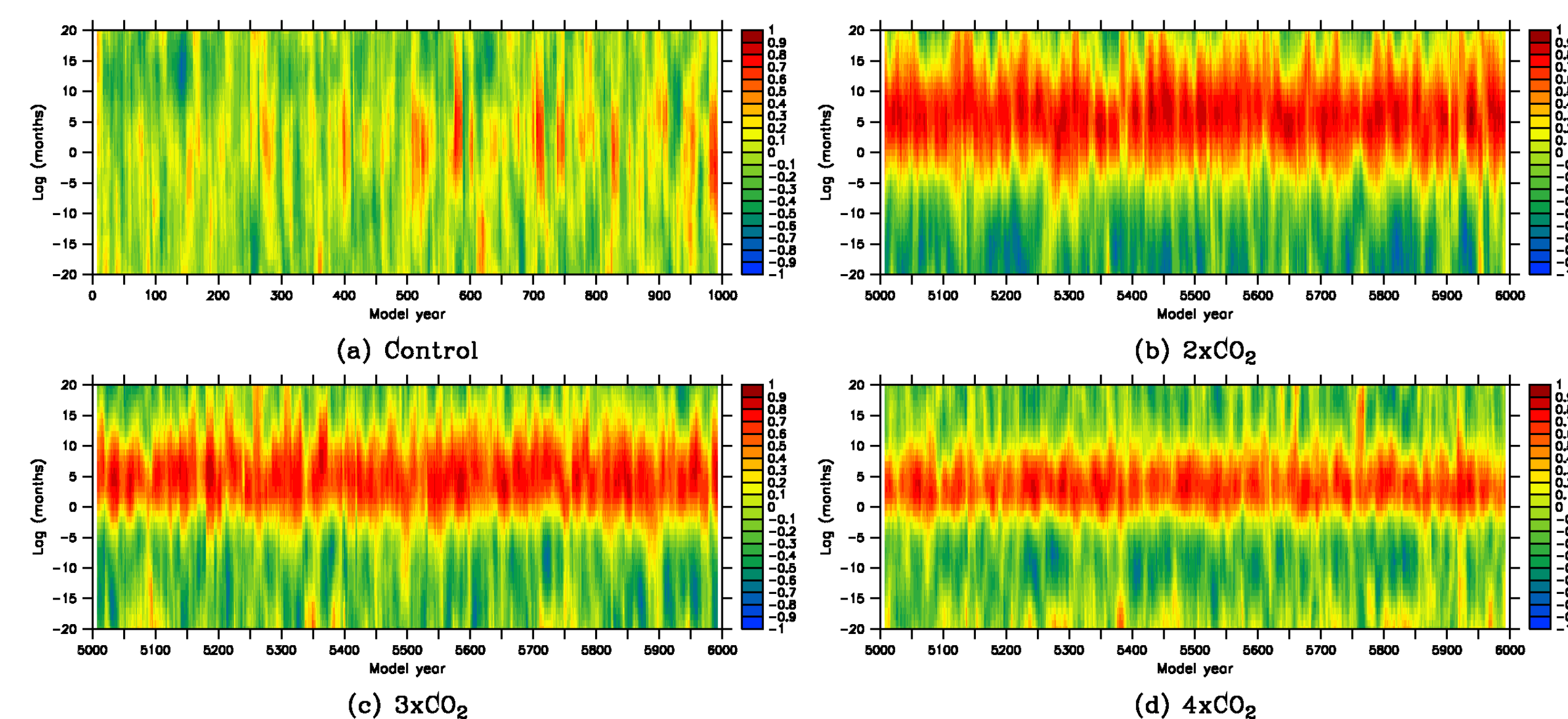


Figure 3. The lag correlation of the Trans-Niño Index (TNI) with the Niño 3 SST anomaly for **a** the control simulation, and **b–d** the equilibrated stages of the 2×, 3× and 4×CO₂ simulations respectively. A negative lag means that the TNI leads, while a positive lag means that the Niño 3 SST leads.

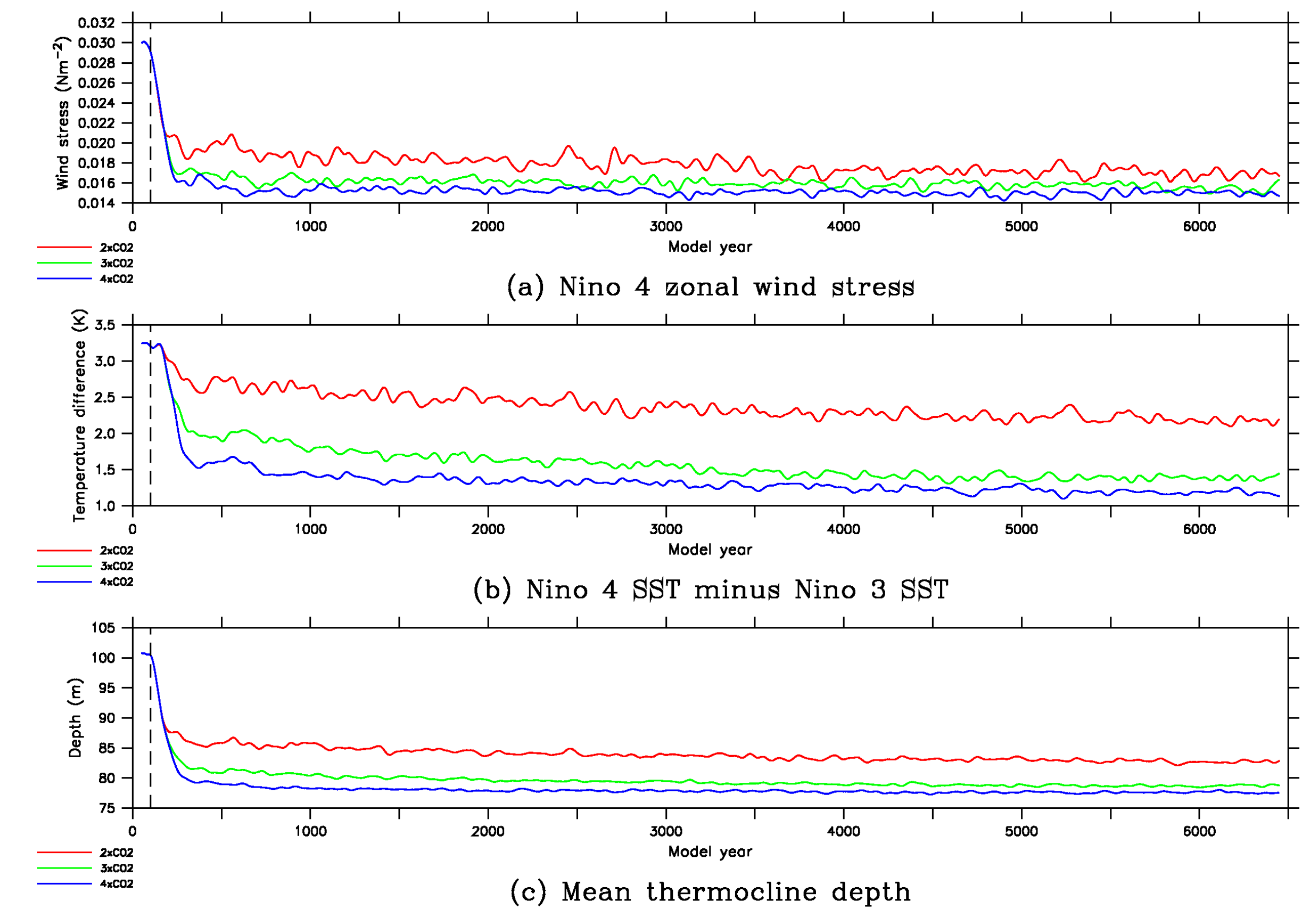


Figure 4. The evolution of **a** the magnitude of the zonal wind stress in the Niño 4 region, **b** the difference between the Niño 4 and Niño 3 SSTs, and **c** the mean thermocline depth in the tropical Pacific. The values plotted have been smoothed using a Hann window with a width of 100 years.

The changes in El Niño behaviour can be understood by examining Figure 4, which shows the evolution in the climate of the tropical Pacific Ocean. The short-term *increase* in El Niño variability is due to changes in the state of the atmosphere. There is a rapid reduction in the strength of the Walker Circulation once the CO₂ concentration begins to increase, as can be seen from Figure 4a. The weaker easterly trade winds make it easier for El Niño events to arise.

The longer-term *decrease* in El Niño variability is due to changes in the state of the ocean. There is a shoaling and flattening of the thermocline in the tropical Pacific, as can be seen from Figures 4b and 4c. The flattening of the thermocline suppresses the development of El Niño events, but does not begin until around 100 years *after* the initial reduction in the strength of the Walker Circulation. This difference in the response timescales of the atmosphere and ocean explains why the *transient* and *equilibrium* changes in El Niño characteristics are different.

5. Conclusions

Using a low-resolution coupled atmosphere-sea ice-ocean general circulation model, it has been shown that the transient and equilibrium responses of El Niño to enhanced atmospheric greenhouse gases can be fundamentally different. As different components of the climate system separately reach equilibrium, the magnitude of El Niño variability can either increase or decrease. This suggests the intriguing possibility that the inter-model differences in ensembles such as AR4 may be due, in part, to differences between the magnitudes of the short- and long-term responses within the models.

6. References

- Guilyardi, E. (2006), El Niño-mean state-seasonal cycle interactions in a multi-model ensemble, *Climate Dynamics*, 26, 329–348.
- Phipps, S. J. (2006), The CSIRO Mk3L Climate System Model, *Technical Report No. 3*, Antarctic Climate & Ecosystems Cooperative Research Centre, Hobart, Tasmania, Australia, 236 pp., ISBN 1-921197-03-X.
- Trenberth, K. E., and D. P. Stepaniak (2001), Indices of El Niño Evolution, *Journal of Climate*, 14, 1697–1701.
- Acknowledgements:* This research was supported by awards under the Australian Research Council's *Discovery Projects* funding scheme (project number DP1092945) and the Merit Allocation Scheme on the NCI National Facility at the Australian National University. The Ferret program was used for analysis and graphics (<http://ferret.pmel.noaa.gov/Ferret/>). Steven Phipps would like to thank the ARC Research Network for Earth System Science for travel support.